KERNFORSCHUNGSANLAGE JÜLICH GmbH
Institut für Plasmaphysik
Association EURATOM-KFA

A Real Time 155 GHz Millimeter Wave Interferometer Module for Electron Density Measurement in Large Plasma Devices

by

P.W. Hüttemann and G. Waidmann

Jül - 1802
September 1982
ISSN 0366-0885

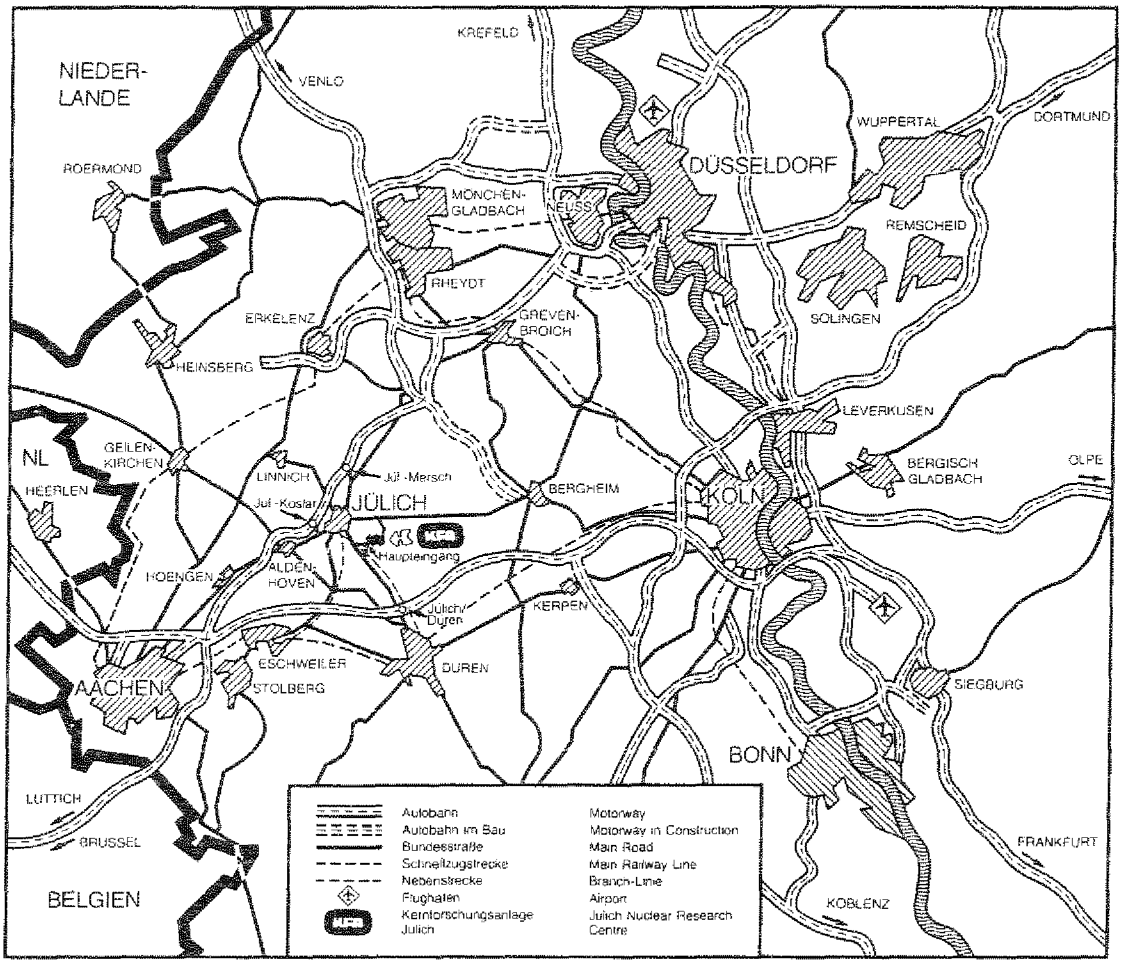

Als Manuskript gedruckt

Berichte der Kernforschungsanlage Jülich – Nr. 1802
Institut für Plasmaphysik Jül - 1802

Zu beziehen durch: ZENTRALBIBLIOTHEK der Kernforschungsanlage Jülich GmbH
Postfach 1913 · D-5170 Jülich (Bundesrepublik Deutschland)
Telefon: 02461/610 · Telex: 833556 kfa d

A Real Time 155 GHz Millimeter Wave Interferometer Module for Electron Density Measurement in Large Plasma Devices

by

P.W. Hüttemann and G. Waidmann

A Real Time 155 GHz Millimeter Wave Interferometer Module
For Electron Density Measurement In Large Plasma Devices.

Abstract

A homodyne, real time 155 GHz interferometer channel is described which is one module of a multichannel system for use on TEXTOR tokamak. A standing sine wave is generated in a phase bridge by transmitting a frequency modulated millimeter wave down two unequal interferometer branches. The presence of plasma produces a phase slip of the sine wave with respect to a reference signal. The phase shift is linear proportional to plasma density for expected TEXTOR plasmas. Long plasma paths give multiradian phase shifts which are recorded by a digital fringe counting system. The accuracy of phase measurement is $\Delta\Phi = 2\pi/16$. Phase changes of $7\pi/8$ are accepted per modulation period. The microwave in the measurement branch of the interferometer is transmitted using a quasioptical technique. Components and technical details are described. The interferometer was tested in a simulation set-up and in two different plasma experiments. Experimental results are presented.

Contents

1. Introduction

Electromagnetic millimeter waves represent a most suitable tool to study electron density and electron temperature in large laboratory plasma devices. In TEXTOR tokamak a continuous monitoring of electron density and temperature with spatial resolution is prepared. Here a transmission interferometric method is described which is used on TEXTOR [1] to measure average electron densities in real time. A 155 GHz carrier wave generated by a small commercial reflex klystron is frequency modulated by electronic means and transmitted through the plasma by means of special antennas. The frequency of the wave was selected so high that under normal operation conditions wave refraction effects can be neglected. A multichannel arrangement is designed for easy and quick installation on a large tokamak machine allowing a splitting of the toroidal vessel and an exchange of vacuum windows when necessary. Since TEXTOR has a heatable vessel (T = 350°C) special windows had to be built for this operation temperature without local cooling of the vacuum system. The easy access to the channels for alignment on the machine and the automatic data acquisition of the interferometer make the millimeter wave system a primary diagnostic instrument for experimental performance.

2. Microwave Ray Propagation Through An Inhomogeneous Plasma

For the propagation of an ordinary millimeter wave $E \parallel B$ through a cylindrical plasma with a density profile refractive effects must be considered. Wave diffraction will be neglected because the parameter $\lambda/2a = 2 \times 10^{-3}$ is rather small for the plasma diameter considered here ($2a = 100$ cm). Also wave damping may be ignored because of the low electron collision frequency compared to the millimeter wave frequency. The ray trajectory of a probing wave depends on the impact parameter r_s/a and the density profile of the plasma. The deflection angle of the trajectory depends critically on the plasma prameter $\omega_p^2 / \omega^2 = n_e/n_c$. Refractive effects are minimized choosing the wave frequency ω sufficiently high with regard to the plasma frequency ω_p.

A survey on the ray trajectory behaviour was attained for typical TEXTOR parameters and assumed density profiles by graphic displays of the trajectories. The differential equation for the ray propagation in an axialsymmetric plasma column can be written as follows [2]:

$$\frac{d(r/a)}{d\Theta} = \frac{r}{a} (\mu^2 V - \mu_s^2 V_s)^{1/2} (\mu_s^2 V_s)^{1/2}$$

The symbols used have the following meaning:

r	=	radius vector of the ray from the plasma center
a	=	radius of the plasma column
Θ	=	angle between the radius vector of the ray and the plasma midplane
μ	=	$(1 - n_e(r)/n_c)^{1/2}$ the plasma index of refraction
v	=	$(r/a)^2$ the reduced radius squared
v_s	=	$(r_s/a)^2$ the reduced impact parameter squared
μ_s	=	$(1 - n_e(r_s)/n_c)^{1/2}$ the plasma index of refraction at the impact parameter r_s.

The differential equation for the ray trajectory was solved numerically as a boundary value problem [3]. Fig. 1 shows in a plot for a parabolic profile the 155 GHz microwave beam trajectories for various impact parameters r_s/a. As a plasma boundary the liner wall is drawn here.

For symmetry reasons only one quadrant of the plasma cross section is plotted. Here an electron density profile

$$n_e(r) = n_o(1 - (r/a)^{2P})$$

with P = 1 was chosen. For a peak density of $n_o = 2 \times 10^{13}$ cm^{-3} there is no essential deviation of the ray. However with increasing density the ray deflection angle becomes noticeable. Fig. 2 shows for a peak electron density $n_o = 1 \times 10^{14}$ cm^{-3} and a parabolic profile this refractive effect.

Different density profiles were tested in Fig. 3. The indices P were varied as P = 0.5; 1; 1.5 and 2. The effect of the density profile on the deflection angle is visible but not very strong. The strongest effect is produced by an increase in peak electron density which can be reduced by an increase in wave frequency.

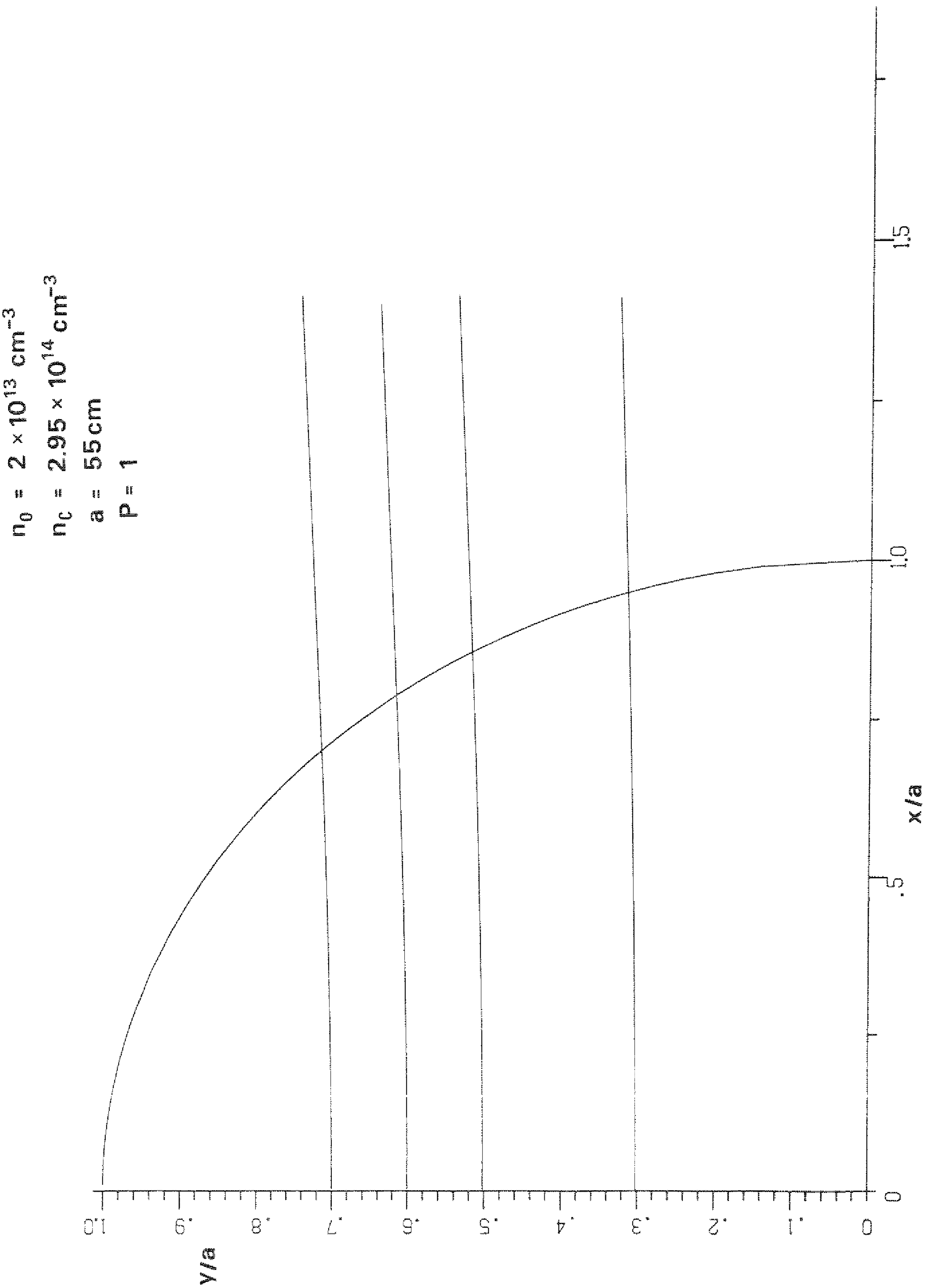

Fig. 1: Ray trajectories of a 155 GHz microwave through a plasma with a parabolic density profile. The peak electron density is $n_o = 2 \times 10^{13}$; the plasma radius up to the liner wall is assumed to be 55 cm. Trajectories are shown for four different impact parameters Y/a.

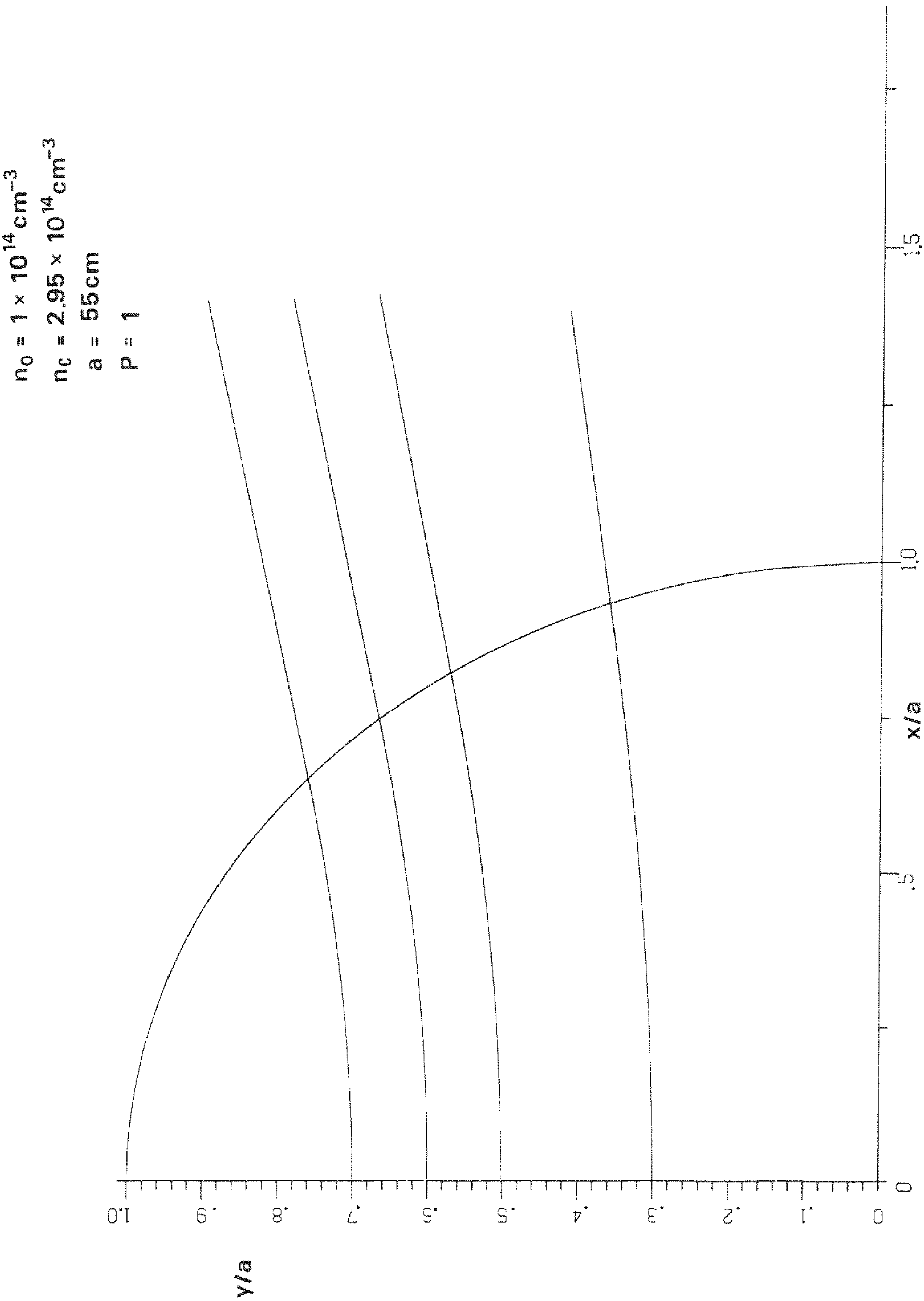

Fig. 2: Ray trajectories through a plasma with a parabolic density profile and peak electron density $n_o = 1 \times 10^{14}$ cm^{-3}. A wave refraction effect is demonstrated.

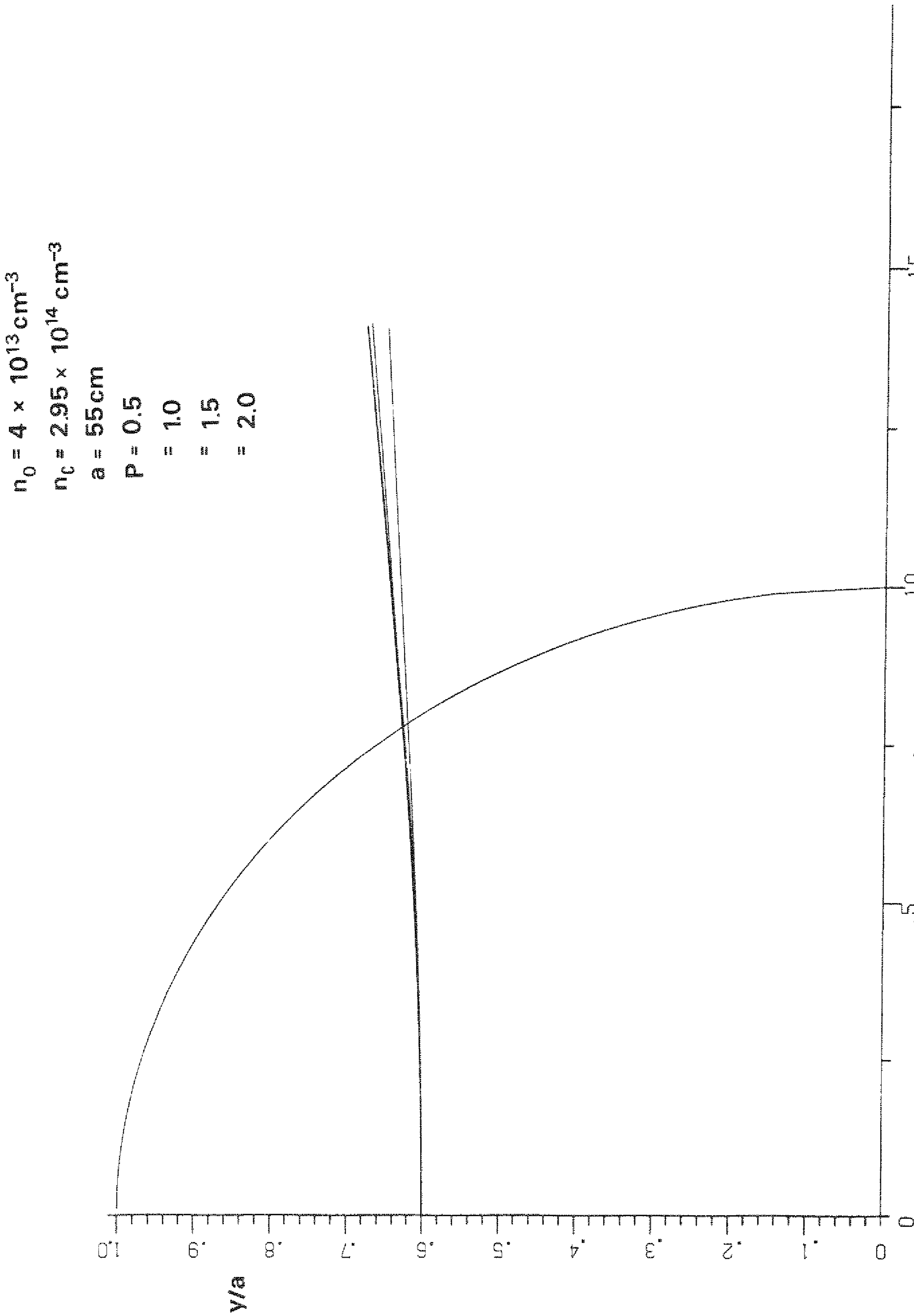

Fig. 3: Microwave ray trajectories through plasmas with different density profile indices: P = 0.5, 1.0, 1.5, 2.0. The peak electron density is $n_o = 4 \times 10^{13}$, the cut-off density for the wave $n_c = 2.95 \times 10^{14}$ cm^{-3}, the impact parameter Y/a = 0.6.

3. Principle Of The Real Time Interferometer.

Several versions of millimeter wave interferometers have been described in the literature [4 - 10]. The basic principle of this real-time interferometer is a single stripe, frequency modulated wave interference set-up. A similar system was recently built for a lower frequency [12]. A millimeter wave E_p with frequency $f_o = 155$ GHz is radiated through the plasma and mixed with a wave E_R of slightly different frequency. This wave originates from the same source but arrives at a mixer over a reference branch (s. Fig. 4). The two interferometer branches have very unequal lengths. The difference in length is $\Delta L = L_p - L_R$; the free space wavelength is λ. The frequency of the source is modulated periodically as

$$f(t) = f_o + \alpha t; \; 0 \leqslant t \leqslant T$$

The two waves arriving at a mixer can be written as follows

$$E_p = \hat{E}_p \, \text{expi} \left\{ 2\pi f_o \left(\frac{L_p}{c} - t\right) + 2\pi\alpha \left(\frac{L_p}{c} - t\right)^2 + \Delta\Phi \right\} \qquad (1)$$

and

$$E_R = \hat{E}_R \, \text{expi} \left\{ 2\pi f_o \left(\frac{L_R}{c} - t\right) + 2\pi\alpha \left(\frac{L_R}{c} - t\right)^2 - \varphi \right\} \qquad (2)$$

The output signal at the mixer is given by the expression

$$I = A + B \cos \left\{ \Delta\omega t + \gamma + \Delta\Phi \, (t) \right\} \qquad (3)$$

assuming a quadratic mixer characteristic. The constants in eq. (3) stand for

$$A = \beta(\hat{E}_p^2 + \hat{E}_R^2)$$
$$B = 2\beta \hat{E}_p \cdot \hat{E}_R$$
$$\Delta\omega = 4\pi\alpha \, \Delta L/c$$
$$\gamma = \varphi + 2\pi f_o \Delta L/c + 2\pi\alpha \, \Delta L(L_p + L_R)/c^2$$

The phase angle φ is introduced by a phase shifter and may be used for a routine check of the interferometer performance. The quantity $\Delta\Phi(t)$ is the phase shift of the probing wave caused by the presence of the plasma and is expressed as

$$\Delta\Phi(t) = \frac{2\pi}{\lambda} \int_L \left\{ 1 - (1 - n_e(Z)/n_c)^{1/2} \right\} dz \qquad (4)$$

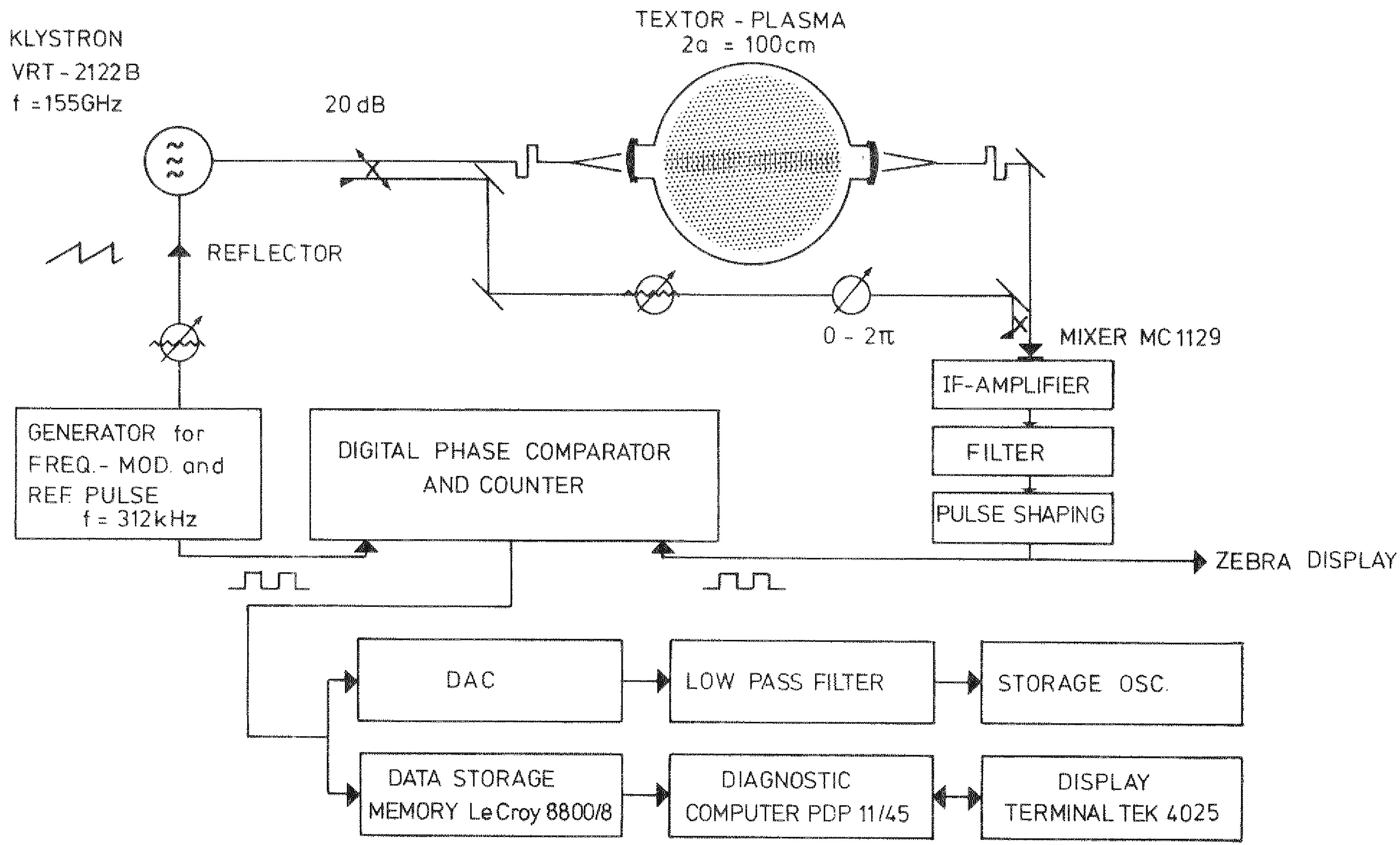

Fig. 4: Schematic diagram of the real time 155 GHz interferometer module.

$n_e(z)$ is the local electron density at position z and $n_c = 3 \times 10^{14}$ cm^{-3} the cut-off density for the 155 GHz millimeter wave. A measurement of this quantity gives an average of the electron density in the open transmission gap.

Without the presence of plasma a sinusoidal oscillation is produced at the mixer by the linear frequency modulation as described by eq. 3. Adjusting now the amplitude and duration of the sawtooth modulation just one oscillation period is observed at the mixer for one modulation cycle of the microwave source. This is reached for $\Delta\omega T = 2\pi$. The occurance of plasma shifts now the phase of this synchronized oscillation. The maximum shift $\Delta\Phi$ during one modulation period T should always be smaller than $\Delta\omega T$ ($\Delta\Phi \ll \Delta\omega T$). The modulation frequency has to be selected for the fastest phase shift i.e. density change expected in the experiment. The integral amount of small phase shifts during consecutive modulation periods will be evaluated by a counting technique.

4. Phase Measurements

A sawtooth modulation frequency of the klystron of 312 KHz was selected. An intermediate frequency of IF = 312 KHz is picked off at a mixer MC1129 (s. Fig. 4). The IF-signal is filtered and pulse shaped. This formed signal contains with regard to the modulation signal the wanted phase information. The time instant of zero-crossing of the IF can be evaluated precisely and an electric needle pulse is derived by differentiation. A visualisation of the phase shift is easily done by an oscilloscope and shown e.g. in the upper curve of Fig. 11. The oscilloscope is swept in the vertical direction by the sawtooth modulation signal and swept in the horizontal by a much lower frequency. The cathode beam is blanked by the voltage spike derived from the zero-crossing. Without plasma a horizontal line is formed by the blanking dots. A phase shift produced e.g. by some artificial means displaces the blanking dots in time. A phase shift of $6.5 \times 2\pi$ is demonstrated in Fig. 11 in a single stripe zebra display. The upper curve in Fig. 11 visualizes that the phase angle $\Delta\Phi$ is not a unique function of the detector output. That is a result of eq. 3. This ambiguity has to be removed yet in an automatized acquisition system.

In Fig. 5 the expected fringe numbers of TEXTOR are shown for an assumed density operation regime. Fringe numbers of the order of 10 and higher will occur and have to be recorded.

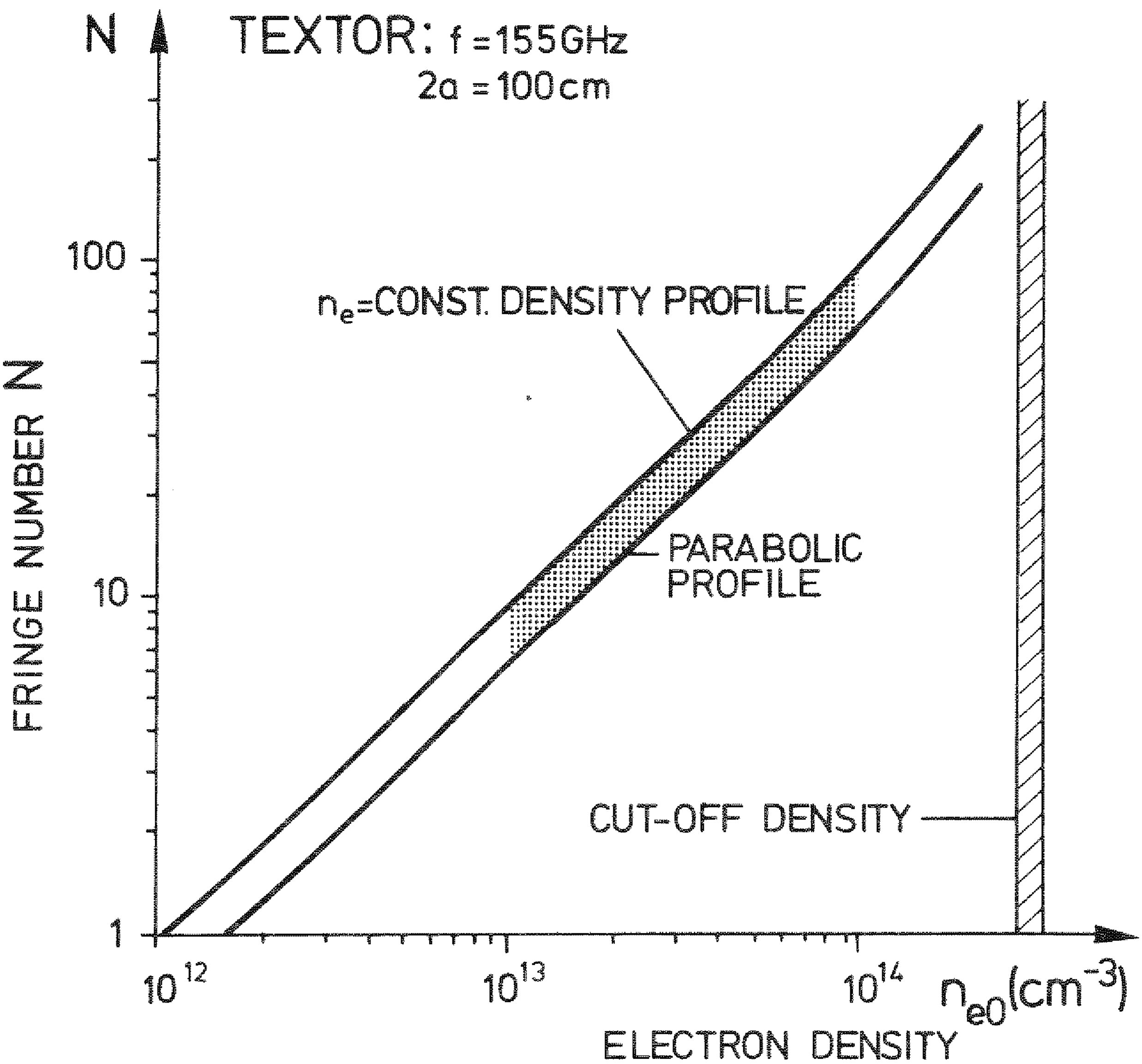

Fig. 5: Fringe numbers calculated for an assumed density operation regime of TEXTOR tokamak.

5. Digital Phase Comparator And Counter

A real time automatic processing by electronic means is needed to acquire the total phase shift of the wave in the measurement branch. The digital circuit employed here is shown in Fig. 6. Two counters measure the time difference between IF-signal from the interferometer and the reference pulse from the modulator. A synchronization circuit controlls the counting period. A 5-MHz oscillator produces a clock at 16 times the 312 KHz IF-frequency. The counters measure a relative phase modulo 16. The phase counters can detect phase differences up to 7/16 x 2π per modulation period. The counting result is buffered and shifted to another buffer after the next counting period. The difference in the buffer status is found by subtraction. The periodic subtraction result is added-up and buffered again. The actual status of the adder can be visualized on monitor after a digital to analog conversion. This counting status is deposited in a memory module, LeCroy 8800. The stored data are transfered from the memory to a diagnostic computer for further data handling. As a Camac logic serves a control board unit from a Le-Croy ADC 8212. Up to 4 memories (= 128 kByte) can be connected. The microwave interferometer channel selection is organized by this Camac unit. The acquisition system permitts the adaption of up to 8 microwave channels.

6. Components And Technical Details

The microwave radiation source is a small commercial reflex klystron VRT-2122B with 60 mWatt output power. It is shown in Fig. 7. The power supply KS-7 used was equipped in addition with an externally clocked 312-kHz sawtooth generator for frequency modulation. The klystron is water cooled by a closed refrigeration cricuit.

For the microwave phase detection a mixer MC 1129 with forward biased GaAs-Schottky diodes is used. The conversion loss of the mixer is 12 dB. The IF-signal of the mixer is amplified by 50 dB. Fig. 8 shows details of the 3 stage low noise IF-amplifier used. The inputs provide a selectable, variable DC-voltage for proper biasing the mixer diodes. The frequency limits of the amplifier were set to 30 kHz resp. 1.5 MHz.

Microwave source and all electronic equipment are mounted in a screened metal cabinet 5 meters away from the center of the tokamak machine. The distance to and from the plasma is bridged by overdimensional waveguide WR 90. The attenuation of the millimeter wave on this waveguide was cut down to 0.3 dB/m. Four 90 degree reflection elements are inserted into the overdimensional guide. Carefully machined H-plane bends were applied exclusively to avoid the excitation of higher order modes known to be produced e.g. by an overdimensional E-plane bend. Linear tapers 75 wavelengths long were installed to maintain the mode pattern which exists in the WR-7 standard waveguide. The other waveguide elements as eg. a 20 dB coupler and an isolator were made on standard waveguide WR-7. No overdimensional beam splitter

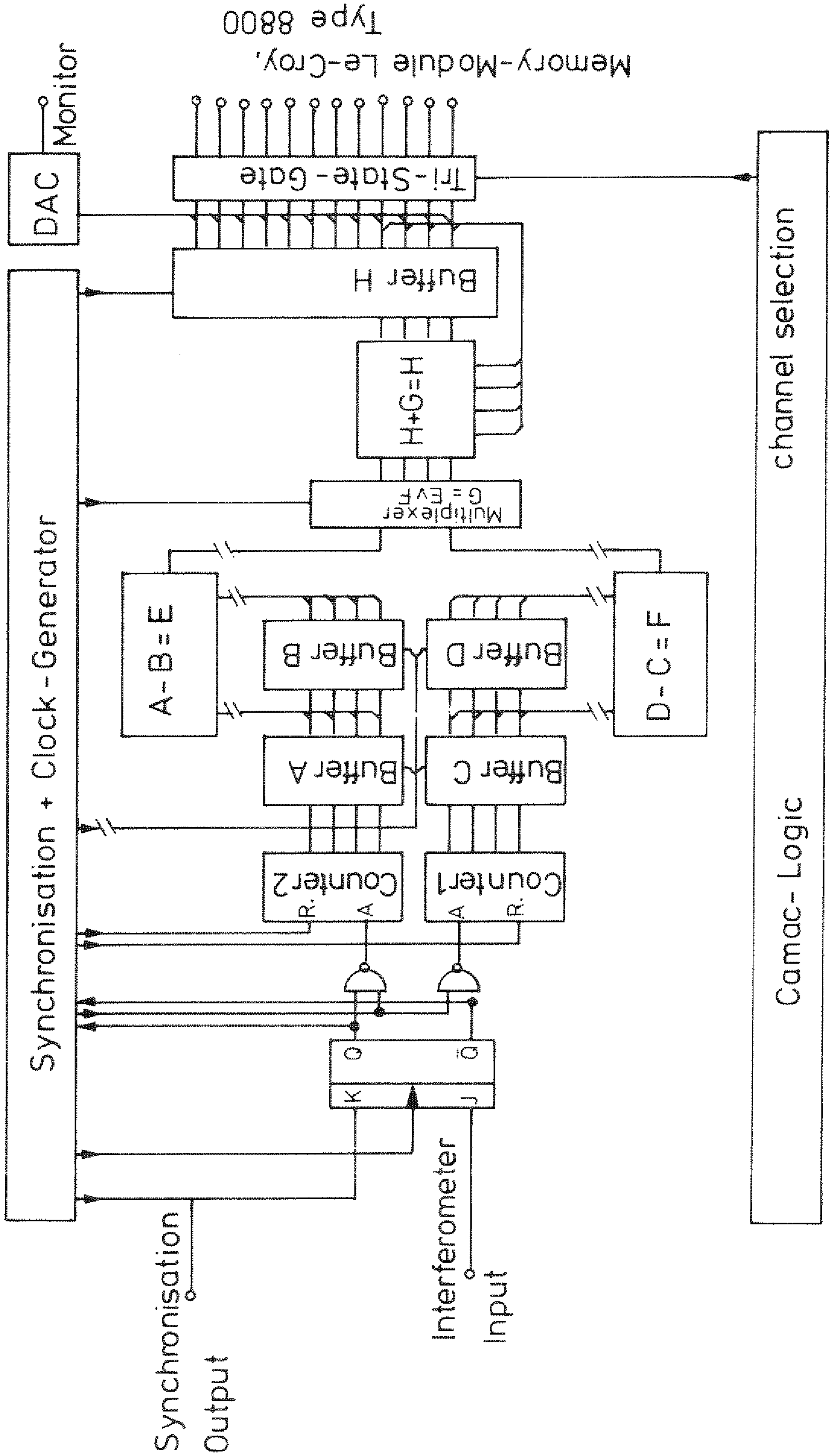

Fig. 6: Schematic representation of the multiradian, digital phase counting and acquisition system.

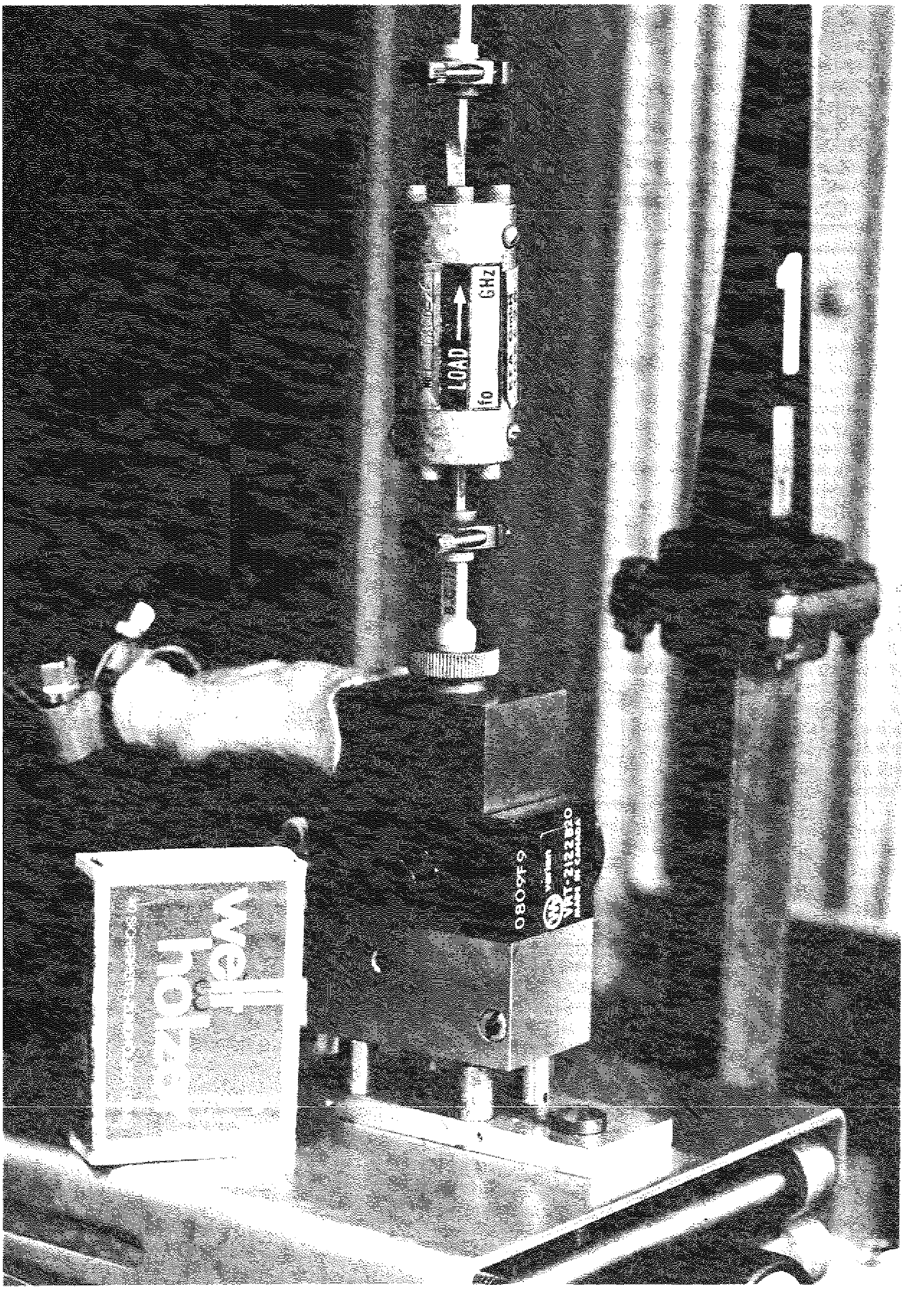

Fig. 7: Reflex klystron with water cooling unit used here as carrier wave generator.

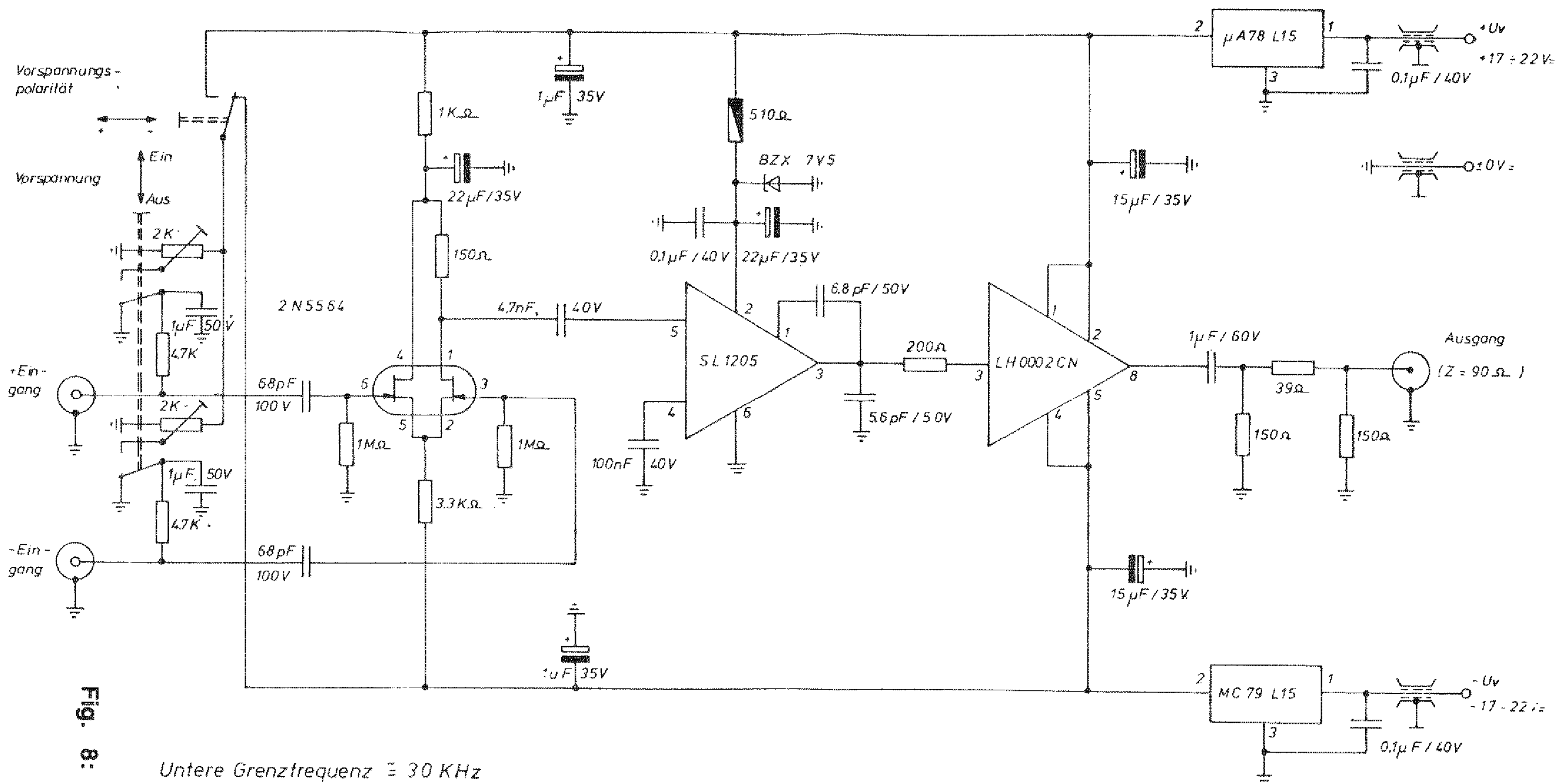

Untere Grenzfrequenz ≅ 30 KHz

Obere Grenzfrequenz ≅ 1,5 MHz

Verstärkung ohne Last ≅ 50 dB

Fig. 8: IF-amplifier circuit.

was used to avoid trapped-mode resonances which could interfere with the fringe counting system. As a consequence each interferometer channel is equipped with its own microwave source. The measurement branch of the interferometer including microwave source, directional coupler, long waveguide WR90, 2 antennas and mixer lie in one plane. A modular microwave channel system results. The different interferometric channels are now completely independent.

An insolation break in the WR-90 waveguide was realised by a thin polyethylene foil. It separates the electronic racks from the tokamak machine area.

Pyramidal horn antennas (s. Fig. 9) with a gain G = 30 dB were fabricated by an electroforming technique. The microwave beam pattern generated by the launching antenna plus microwave window was measured at a distance which corresponds to the center of the vacuum vessel. Fig. 10 shows the beam profile 90 cm in front of the antenna. The beam waist (3 dB points) has a diameter of 4 cm.

The heatable vessel of TEXTOR requires bakeable microwave windows. Aluminumoxyd was found a suitable material from the point of microwave absorption loss. It can be machined and brazed to vacuum compatible material. Microwave windows with a diameter of 10 cm were built as lenses to focus slightly the microwave beam into the vessel center and to reduce transmission losses in the vessel. Fig. 11 shows a drawing of the microwave window mounted in a CF-100 flange.

7. Testing Procedure

A 1:1 mockup of the TEXTOR vacuum vessel cross section was built in the laboratory to test the performance of components and electronics. The microwave beam cross section in the center of the vessel was generated by the mentioned high directivity horns and focusing ceramic windows. The beam profile was evaluated by a small horn antenna which was moved with constant speed across the beam diameter.

A plasma was periodically simulated in the center of the vessel by means of a rotating dielectric double wedge. The transit of this dielectric object through the beam produces at first a linear phase shift of the wave up to 6.5 x 2π. The following second part of the dielectric with constant thickness does not change the phase. The second wedge with decreasing thickness reduces the integrated phase shift down to zero. Fig. 12 shows the dielectric object simulating the three phases of a pulsed plasma and the corresponding phase shift ($\Delta\Phi = 13\pi$ at the plateau) visualised here by blanking the cathode of an oscilloscope when the IF crosses zero. The lower oscilloscope trace gives the real time output of the counting circuit after DAC conversion. The continuous operation of the interferometer showed the importance of frequency stabilization of the klystron against thermal excursions leading to frequency drifts and perturbations of the IF-signal.

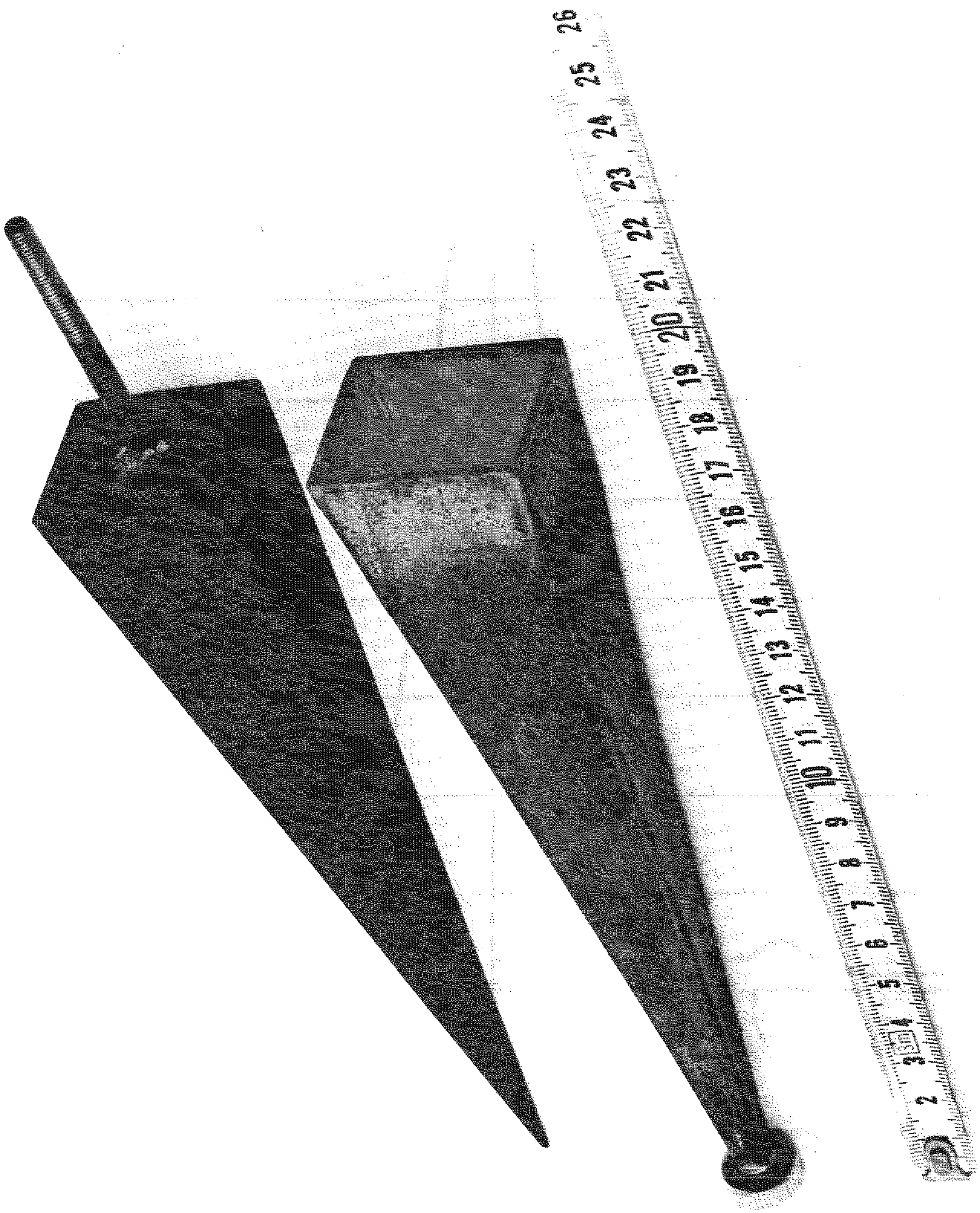

Fig. 9: High directivity horn antenna fabricated by electroforming technique.

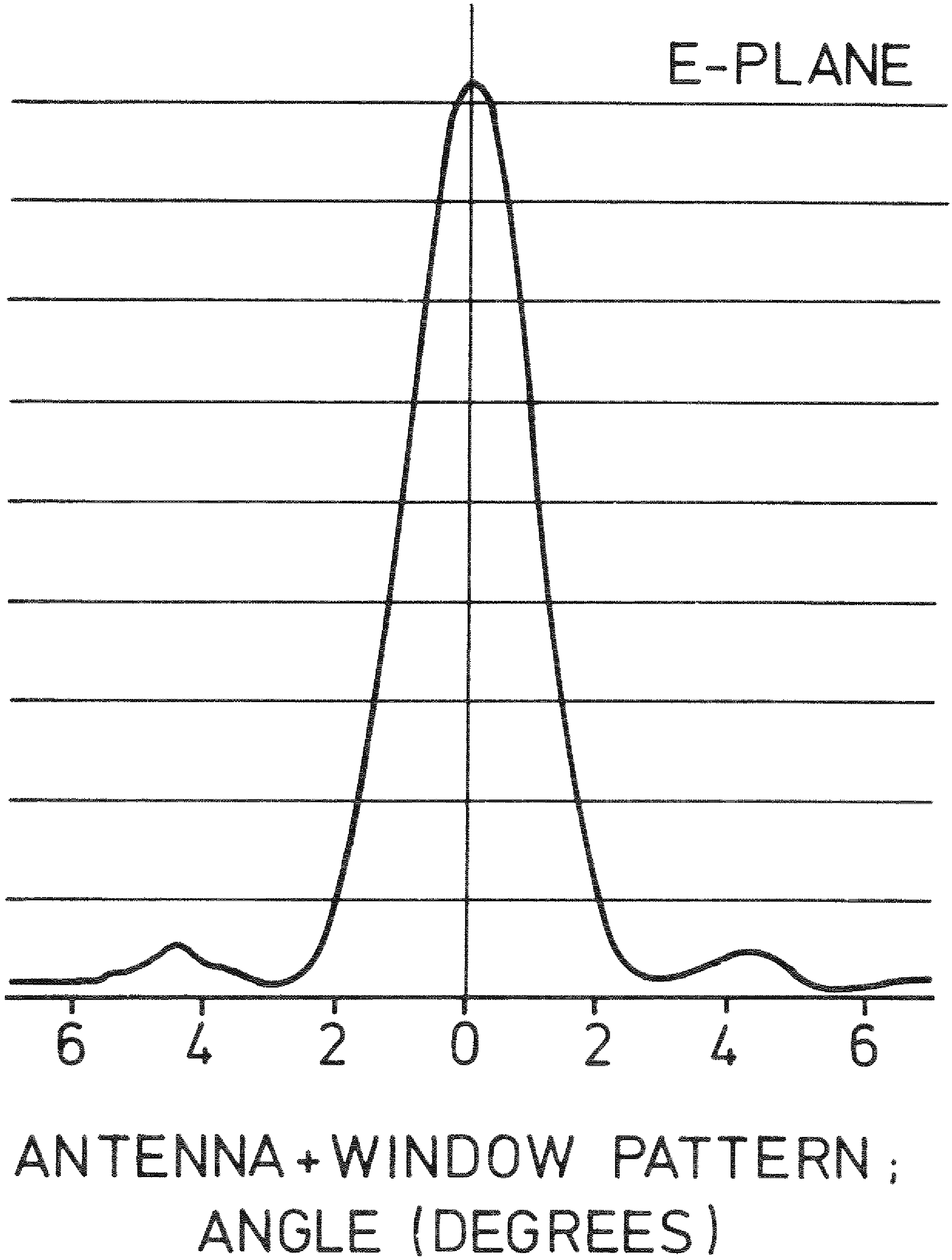

Fig. 10: Microwave probing beam profile in the center of the vacuum vessel; E-plane pattern.

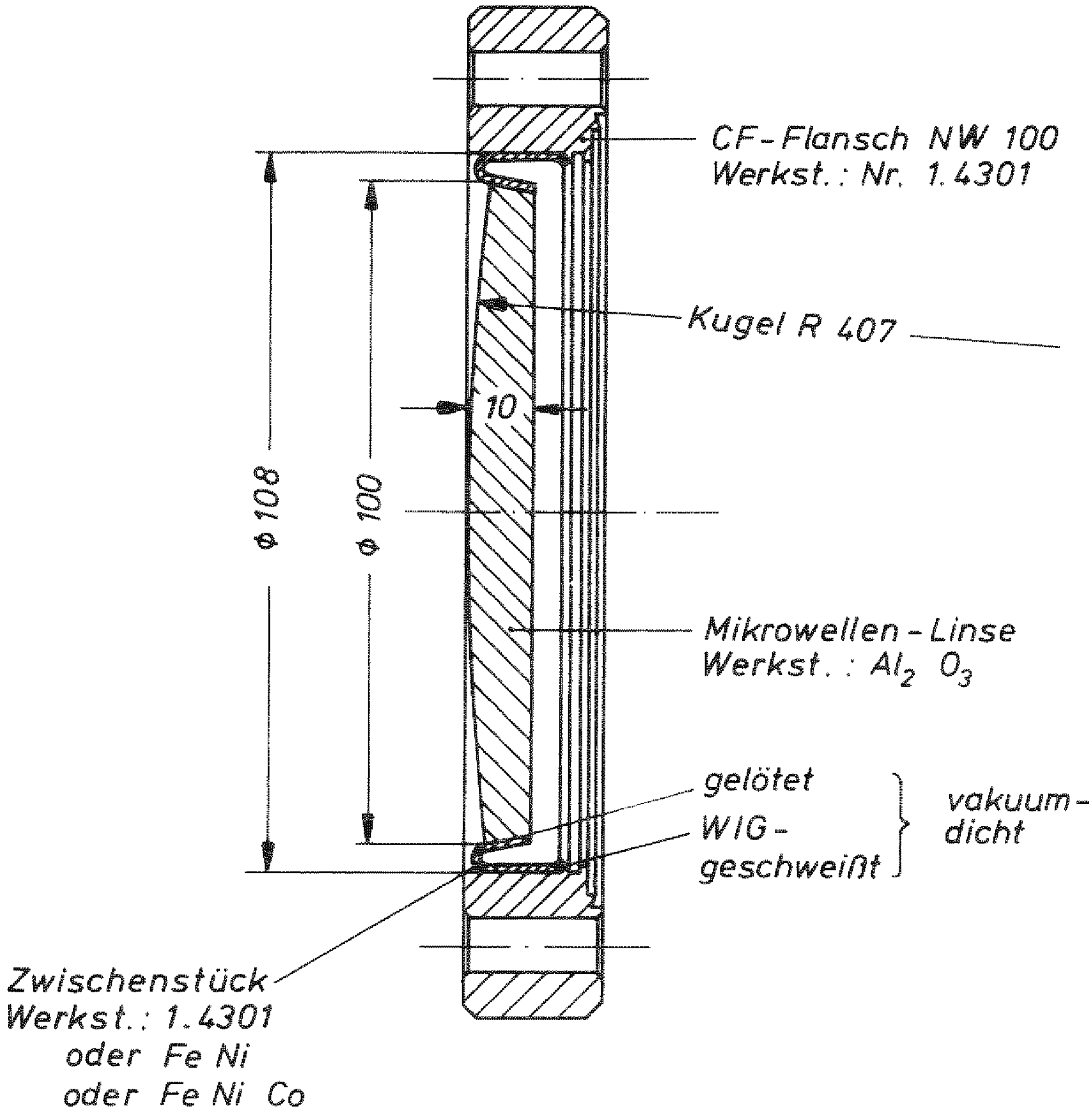

Fig. 11: Bakeable aluminumoxyd window mounted into a CF-100 flange. The window represents a focusing ceramic lens.

8. Density Measurements On Plasma Experiments

A second test of the interferometer was performed on a pulsed, electrodeless, toroidal plasma with a major radius R = 25 cm and a minor radius a = 10 cm [13]. The interferometer response to a short, transient plasma is demonstrated in Fig. 13. Only a phase shift of one fringe is generated here by a low density plasma corresponding to an average density of $n_e = 5 \times 10^{12}$ cm^{-3}. This density increase is resolved in 40 μsec. A faster density rise would soon lead to counting errors of the electronic system. The upper trace shows the registration pulses superimposed on the modulating reflector voltage. The middle trace shows the DAC signal which corresponds to 1 fringe and represents a line density $n_e \times L = 10^{14}$ cm^{-2}. The lower trace represents an oscillating magnetic field which induces the plasma in the toroidal vessel. For a linear rising density a density growth rate of 25 fringes per millisec should be detectable with the present system. Higher growth rates require a shorter modulation period of the microwave oscillator which is still possible.

The 155 GHz system then was operated on TEXTOR-tokamak [14]. The free microwave transmission gap was now 180 cm, the plasma diameter 100 cm. Fig. 14 shows a hardcopy from a terminal display of a TEXTOR discharge. The lifetime of the plasma was 1.2 sec and the plasma current amplitude was $I_p = 200$ kA. The fringe counting gave 10 fringes at the density maximum. This corresponds to an average electron density $n_e = 10^{13}$ cm^{-3}. The averaging is taken over the beam path through the plasma, here over 2a = 100 cm.

Fig. 15 shows the density behaviour of an unstable discharge which terminated after 140 msec with a hard current disruption. A rather smooth density rise is observed during density built-up in the first 30 msec. However strong density fluctuations are seen in the late phase of the discharge before disruption.

Acknowledgements

The authors wish to acknowledge the work of Mrs. R. Klein, Mr. J. Neander, W. Pysik and J. Stiel during the development of components and the testing of the complete system.

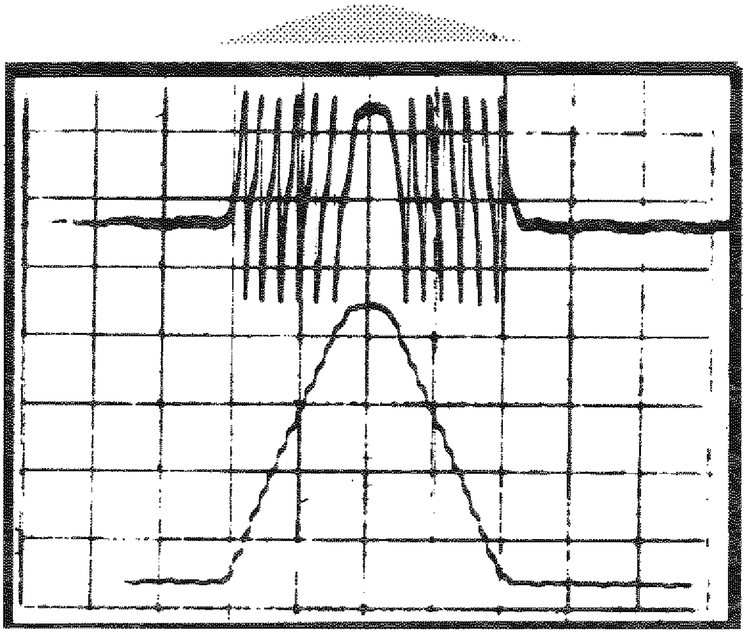

Fig. 12: Results of a simulation test are shown. A dielectric double wedge (top) is rotated through the microwave beam. The phase shift produced by the dielectric is given by the upper trace. The curve represents Sin $\Delta\Phi(t) \propto \mathrm{Sin}(n_e(t))$. A maximum shift of 13π is recorded. The lower curve shows the unique display as recorded by the digital phase counter after DA-conversion. The sweep speed of the oscilloscope was 20 msec/cm.

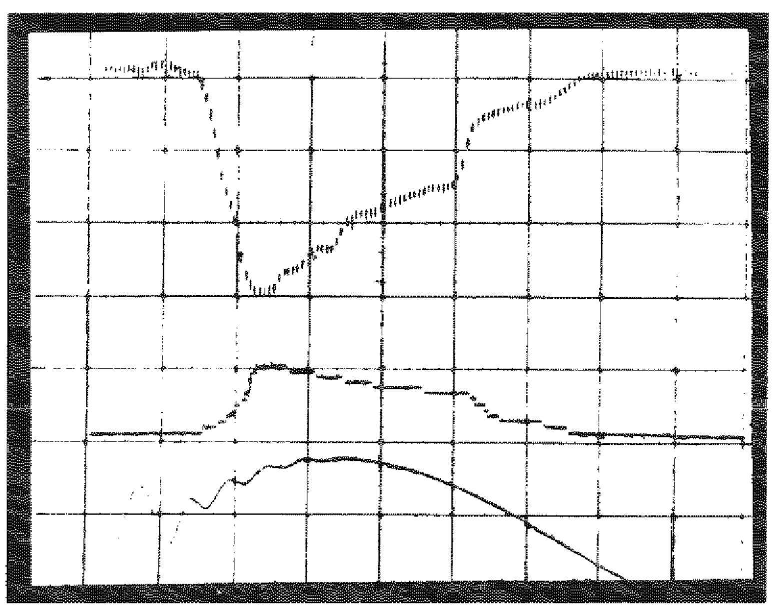

Fig. 13: Single stripe zebra display (upper trace: Sin $\Delta\Phi$) and real time interferometer output (middle trace: $n_e(t)$) recorded on a small pulsed toroidal discharge. The lower trace shows an oscillating magnetic field. The sweep speed here was 50 μsec/cm. A phase shift of 2π was produced by this transient plasma. It corresponds to a plasma line density $n_e = 10^{14}$ cm^{-2} at maximum density.

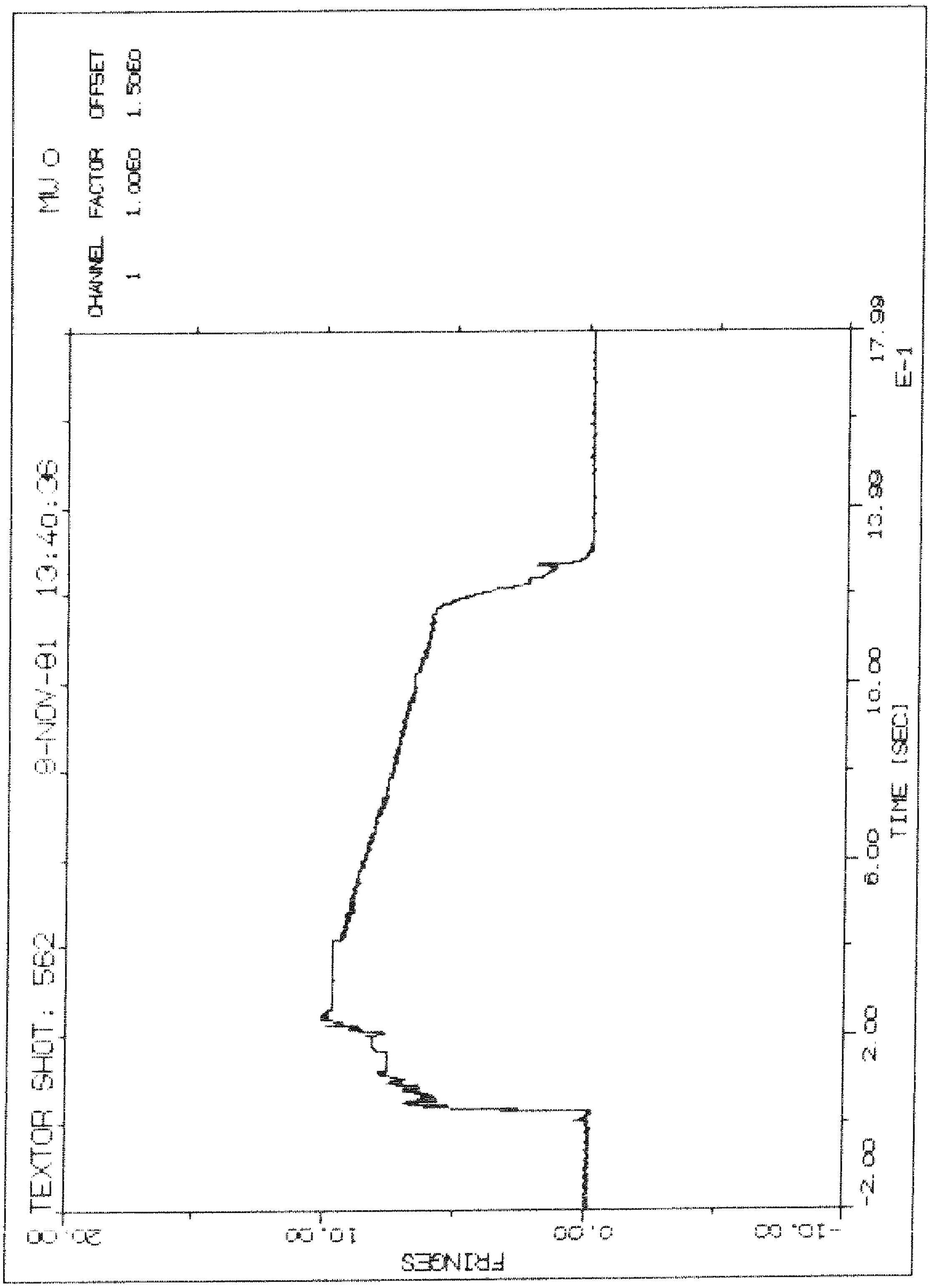

Fig. 14: Average electron density of a TEXTOR discharge with I_p = 200 kA as a function of time. The maximum fringe number N = 10 corresponds to an average density n_e = 10^{13} electrons/cm^3

9. References

[1] H. Conrads
"TEXTOR"; 10th Symposium on Fusion Technology, Padua, 1978, Paper A1

[2] J.C. Hosea and F.C. Jobes
Multichannel Wave Interferometry, Report MATT-1176 (1975)

[3] G. Waidmann
Interferometric Plasma Position Detection in Tokamak Experiments; Report JÜL-1579, Febr. 1979

[4] M.A. Heald and C.B. Wharton
Plasma Diagnostics With Microwaves (J. Wiley 1965) Chap. 6

[5] J.P. Crenn
Etude de la Mesure de Densite Electronique du Plasma de Tokamak-FAR par Interferometrie Microonde, Report EUR-CEA-FC-608 Aug. 1971

[6] C.A.J. Hugenholtz and A.J. Putter
Microwave Interferometer with Digital Read-Out for Large Numbers of Fringes. Rijnhuizen Report 73/81, Sept. 1973

[7] B.J.H. Meddens and R.J. Taylor
A Multiradian MM-Interferometer, Rijnhuizen Report 74-85 (1974)

[8] G. Lisitano, P. Morandi, B. Cannici, E. Rossetti, N. Gottardi
Density Distribution Measurements in Large C.T.R.-Devices. Report MPI-Garching, IPP III/17 May 1975

[9] K. Matsuura, J. Fujita, A. Ogata, K. Haba
Direct Reading Type Microwave Interferometer Report IPP-J-T-29, Oct. 1977

[10] R. Bitzer, W. Ernst and G. Cutsogeorge
PDX Multichannel Interferometer, Report PPPL-1714, Oct. 1980

[11] P.W. Hüttemann, G. Waidmann
A Real Time 155-GHz Microwave Interferometer for Remote Electron Density Measurements in Large Plasma Devices. 10th Europ. Microwave Conf. Proceedings, Warszawa 1980, paper MSI.4 p. 251.

[12] M. Durvaux
Realisation d'un Interferometre Multicanal; Report EUR-CEA-FC-1009, June (1979)

[13] F. Sand, F. Waelbroeck, G. Waidmann
Preionisation and Preheat Conditions for a Compact Toroidal Plasma, Nuclear Fusion 13, 373 ff (1973)

[14] TEXTOR-Team, G. Waidmann
First Results of Magnetic Diagnostics during Commissioning of TEXTOR, Spring-Meeting of the DPG, Würzburg 1982, Paper P1.